J. Am. Soc. Mass Spectrom. (2015) 26:1559–1569
DOI: 10.1007/s13361-015-1160-8

RESEARCH ARTICLE

Iron Fluoroanions and Their Clusters by Electrospray Ionization of a Fluorinating Ionic Liquid

Christopher A. Zarzana,[1] Gary S. Groenewold,[1] Michael T. Benson,[1] James Delmore,[1] Tetsuya Tsuda,[2] Rika Hagiwara[3]

[1]Idaho National Laboratory, Idaho Falls, ID 83415-2208, USA
[2]Department of Applied Chemistry, Graduate School of Engineering, Osaka University, Osaka, Japan
[3]Department of Fundamental Energy Science, Graduate School of Energy Science, Kyoto University, Kyoto, Japan

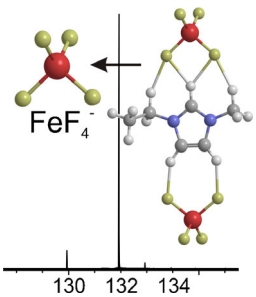

Abstract. Metal fluoroanions are of significant interest for fundamental structure and reactivity studies and for making isotope ratio measurements that are free from isobaric overlap. Iron fluoroanions $[FeF_4]^-$ and $[FeF_3]^-$ were generated by electrospray ionization of solutions of Fe(III) and Fe(II) with the fluorinating ionic liquid 1-ethyl-3-methylimidazolium fluorohydrogenate $[EMIm]^+[F(HF)_{2.3}]^-$. Solutions containing Fe(III) salts produce predominately uncomplexed $[FeF_4]^-$ in the negative ion spectrum, as do solutions containing salts of Fe(II). This behavior contrasts with that of solutions of $FeCl_3$ and $FeCl_2$ (without $[EMIm]^+[F(HF)_{2.3}]^-$) that preserve the solution-phase oxidation state by producing the gas-phase halide complexes $[FeCl_4]^-$ and $[FeCl_3]^-$, respectively. Thus, the electrospray-$[EMIm]^+[F(HF)_{2.3}]^-$ process is oxidative with respect to Fe(II). The positive ion spectra of Fe with $[EMIm]^+[F(HF)_{2.3}]^-$ displays cluster ions having the general formula $[EMIm]^+_{(n+1)}[FeF_4]^-_n$, and DFT calculations predict stable complexes, both of which substantiate the conclusion that $[FeF_4]^-$ is present in solution stabilized by the imidazolium cation. The negative ion ESI mass spectrum of the Fe-ionic liquid solution has a very low background in the region of the $[FeF_4]^-$ complex, and isotope ratios measured for both $[FeF_4]^-$ and adventitious $[SiF_5]^-$ produced values in close agreement with theoretical values; this suggests that very wide isotope ratio measurements should be attainable with good accuracy and precision when the ion formation scheme is implemented on a dedicated isotope ratio mass spectrometer.

Keywords: Ionic liquid, Fluoroanion, Electrospray, Fluorohydrogenate, Isotope ratio

Received: 19 September 2014/Revised: 19 March 2015/Accepted: 29 March 2015/Published Online: 8 May 2015

Introduction

Fluoroanions have been the subject of a range of fundamental and applied research because they have extensive potential for useful fluorination chemistry and also provide a means for studying fluorine interactions with Lewis acids such as metal cations. For example, fluoroanions can be used to probe new bonding motifs in organometallic complexes, involving metals that include B [1], Co [2–6], Ga [7], As [1], Cd [8], Pd [9], In [7], Sn [10], and U [11]. One of the most intriguing properties of fluoroanion-containing materials is the ability to solvate HF, which has the potential to provide improved safety and efficiency for synthetic chemistry [7, 11–28]. For example, anhydrous HF-containing systems have great utility for synthesis of high oxidation state fluoroanions, such as $[AgF_4]^-$ and $[NiF_6]^{2-}$ [29], and the extensive research of Hagiwara and coworkers has shown that HF stabilized in ionic liquids can be used to make a variety of fluoroanions, including $[BF_4]^-$, $[PF_6]^-$, $[AsF_6]^-$, $[SbF_6]^-$, $[NbF_6]^-$, $[TaF_6]^-$, and $[(FH)_{2.3}F]^-$ [20]. These approaches build upon established approaches, such as using trimethylamine with fluoromethane with the appropriate Lewis acid to synthesize BF_4^-, PF_6^-, SiF_5^-, SiF_6^{2-}, GeF_5^-, and GeF_6^{2-} [30], and the more exotic use of high oxidation state binary transition metal fluorides as fluorinating agents [31].

Determination of fluoroanion composition and structure has utilized both NMR and X-ray approaches. An excellent example of the former are ^{19}F NMR investigations of Sb

Electronic supplementary material The online version of this article (doi:10.1007/s13361-015-1160-8) contains supplementary material, which is available to authorized users.

Correspondence to: Gary Groenewold; *e-mail:* gary.groenewold@inl.gov

fluoroanions as conjugates with HSO_3F [32] and in HF-SbF_5 systems [33]. X-ray crystallography has been used to determine the structures of hexamethylpiperidinium salts of $[IF_2]^-$, $[ClF_4]^-$, $[IF_4]^-$, $[TeF_7]^-$, and $[AsF_4]^-$ [34]. Extended X-ray absorption fine structure is also highly useful, for example investigations of metal fluoride bonds of singly and doubly charged hexafluoroanions of Ru, Rh, and Pd [35], and Os, Ir, and Pt [36]. Accurate measurement of the unit cell volumes of lithium salts of singly and doubly charged hexafluoroanions of Nb, Ru, Rh, Ta, Os, Ir, Pt, and Au were measured using synchrotron X-ray powder diffraction studies [37]. In contrast, there have been far fewer investigations of fluoroanion species in the gas phase. Several prior investigations of gas-phase metal fluoroanions have been motivated by the need to measure isotope ratios without isotopic overlap. Measurements of trace isotopes of many elements have been limited because they require formation as anions, which is a practical requirement for accelerator mass spectrometry. This is normally accomplished by compounding the metal of interest with oxygen, which, while effective, introduces isobaric overlap problems stemming from the two minor isotopes ^{17}O and ^{18}O. Litherland and coworkers have noted this and recently canvassed the periodic table, demonstrating that sputter ionization of a PbF_2 matrix can be used to form metal fluoroanions [38–40]. The MF_n^- species that were formed in this manner generally contained element M in the oxidation state most prominent in the condensed phase.

The fact that fluoroanions can be produced in ionic liquids (ILs) suggests negative-mode electrospray ionization (ESI) as an alternative means of producing gas-phase metal fluoroanions. A number of groups have shown that ESI can be used to investigate ionic liquids, despite their famously low vapor pressure; ion pair evaporation was demonstrated by Hogan and de la Mora, which explains how these materials are compatible with ESI-MS [41]. Some of the initial ESI studies analyzed neat ionic liquids for contaminants, which could be accomplished using a heated curtain gas [42], or by merely placing a droplet in the flow of the desolvation gas [43]. The low vapor pressure of the ionic liquids enabled vacuum ESI-MS studies of imidazolium ionic liquids from a tungsten emitter [44, 45], and investigations of ESI of ILs as sources of cluster ions [46–49].

Finding degradation products has been a common objective for ESI studies of ILs, for example measurement of hexafluorophosphate degradation products caused by electrolysis of water [50], or radiolysis products [51]. Normally, ESI-MS studies are conducted by diluting the ILs in polar or even nonpolar solvents [42, 52]. Generally the ESI response for IL components and solutes is intense, so ESI has been used in a wide range of analytical studies, including measuring the solubility of ILs in water [53], the compositions of strontium [54] and uranyl [55] coordination complexes, and the compositions of Rh and Ru complexes used as catalysts [56, 57]. Facile ESI production of IL-derived ion pairs was used to measure relative anion–cation binding energies by collision induced dissociation reactions that displayed trends similar to those generated using density functional theory (DFT) calculations [58].

These studies suggested that abundant fluoroanions might be produced by ESI of the fluorinating ILs, and this proved to be the case. Solutions of a fluorinating ionic liquid 1-ethyl-3-methylimidazolium fluorohydrogenate $[EMIm]^+[F(HF)_{2.3}]^-$ produced abundant $[SiF_5^-]$ by ESI, which was formed by interaction of the IL with the fused silica capillary feeding the electrospray capillary [59]. $[EMIm]^+[F(HF)_{2.3}]^-$ was originally developed by Hagiwara and coworkers [13–18, 20, 22, 24, 25] with the objective of generating a fluorinating environment for organic fluorination reactions [26–28]. The formula of this IL implies that on average, 2.3 HF molecules are complexed for each fluoride anion, forming a new liquid that is largely vacuum stable. Both $[F(HF)_2]^-$ and $[F(HF)_3]^-$ are present in the fluorohydrogenate IL; however, these anions can be replaced by $[BF_4]^-$, $[PF_6]^-$, $[AsF_6]^-$, $[NbF_5]^-$, $[TaF_5]^-$, and $[WF_7]^-$ when these metals were present [19, 21, 23]. Subsequent studies focused on zirconium and showed that $[ZrF_5]^-$ and $[ZrF_6]^{2-}$ were produced by treating Zr^{4+} or ZrO^{2+} salts with $[EMIm]^+[F(HF)_{2.3}]^-$ [60]. The Zr fluoroanions were observed by diluting the IL-Zr solutions in acetonitrile and electrospraying the resulting solutions.

In this report, we describe formation of $[FeF_4]^-$; iron was investigated because unlike Zr or Si, it has two easily accessible oxidation states, and it is of interest whether electrospray of the ionic liquid-metal solution would preserve the oxidation state of iron originally present in solution. In addition to addressing ion formation questions, the iron fluoroanions might have utility for isotope ratio measurements; since fluorine is monoisotopic, the isotopic envelope of the iron fluoroanions reflects only the iron isotope ratio.

Experimental

Iron Chloride Solutions

$[EMIm]^+[F(HF)_{2.3}]^-$ was generated according the method of Hagiwara by condensing anhydrous HF onto 1-ethyl-3-methylimidazolium chloride [13]. A nominal 10 mM solution of $[EMIm]^+[F(HF)_{2.3}]^-$ in LC-MS grade acetonitrile (Fisher Scientific, Pittsburg, PA, USA) was made by dissolving 10 μL of the ionic liquid in 5398 μL of solvent. Aqueous solutions of $Fe(II)Cl_2$ and $Fe(III)Cl_3$ (each at 10 mM) were prepared from nanoPure water. Iron chloride/acetonitrile solutions were prepared by mixing the aqueous iron chloride solutions with LC-MS grade acetonitrile in a 1:9 ratio to produce approximately 1 mM iron chloride in a 9:1 acetonitrile:water solvent. Solutions containing iron chloride and the ionic liquid were prepared by mixing the aqueous iron chloride solutions with 10 mM $[EMIm]^+[F(HF)_{2.3}]^-$ in acetonitrile in a 1:9 ratio to produce approximately 1 mM iron chloride and 9 mM $[EMIm]^+[F(HF)_{2.3}]^-$ in the 9:1 acetonitrile:water solvent. In one experiment, an aliquot of the aqueous iron(III) chloride solution was treated with approximately 1000 molar equivalents of hydrogen peroxide relative to Fe to ensure all of the iron in solution was iron(III) prior to mixing with pure acetonitrile.

Electrospray Ionization Mass-Spectrometry (ESI-MS)

Electrospray-ionization mass spectra were collected using a microTOF-Q II (Bruker, Billerica, MA, USA). Samples were injected via direct infusion into the ESI-MS at a rate of 3 μL/min, using a syringe pump (KD Scientific, Holliston, MD, USA). The ESI dry gas (desolvation gas as sheath gas for the ESI droplets) temperature was 180 °C, and operated at a flow rate of 4 L/min. Electrosprayed ions were transferred from the ESI source to the acceleration region of the time-of-flight mass analyzer via a capillary transfer tube, two serial ion funnels, a hexapole, a quadrupole, and a collision cell. For single-stage mass spectrometry, the quadrupole was operated in an rf-only mode. For MS/MS experiments, it operates as a mass filter for selecting the parent ion of interest prior to collision induced dissociation occurring in the collision cell. Nitrogen was used as the collision gas, at a pressure of about 1×10^{-2} mbar. Ion energies in the MS/MS experiments were on the order of 20–60 eV (E_{lab}): excitation energy is imposed by applying a potential to the collision cell as a percentage of the maximum value, which was 200 eV. In the experiments shown, fragmentation was achieved by applying 10%–30%. Ion elemental composition can be deduced by way of accurate mass measurement, which is facilitated by the mass resolution of the instrument (~8000 m/Δm). Mass measurement accuracy of about 5 ppm is achievable using external calibration. The mass spectrometer was operated using standard Bruker tuning parameters, specifically "tune low" (see Supplementary Material Tables S1 and S2).

Computational Methods

Gaussian03 was used for optimization of all molecular geometries and vibrational analyses [61]. Density functional theory [62] calculations were performed at the B3LYP level of theory [63, 64], with the 6-311++G(d,p) basis set for all atoms. Calculations were initiated starting from a variety of structures that were generated by intuition and previous experience with similar zirconium–ionic liquid complexes [60]. All calculated structures are true minima (i.e., no imaginary frequencies). Coordinates for all calculated structures are provided in Table S3 in the Supplemental Material.

Results and Discussion

Analysis of Iron(III) and Iron(II) Chlorides Dissolved in [EMIm][F(HF)$_{2.3}$]

The negative electrospray ionization mass spectrum of a solution of $FeCl_3$ dissolved in water and then diluted with 10 mM $[EMIm]^+[F(HF)_{2.3}]^-$ ionic liquid in acetonitrile contained an intense ion at *m/z* 132 that corresponds to $[FeF_4]^-$ (Figure 1), in which the oxidation state of iron is preserved at +3 upon going from the condensed phase to the gas phase. In this experiment, fluoride has replaced chloride as the ligand on the Fe metal center in an almost quantitative fashion. The only hint of chloride in the strictly inorganic clusters is seen at *m/z* 148, which corresponds to $[FeClF_3]^-$, but this has a relative abundance of <1%. A low abundance ion at *m/z* 113 is ascribed to the Fe(II) species $[FeF_3]^-$, which most likely arises as the product of a low-efficiency ionic fragmentation reaction, supported by the collision-induced dissociation (CID) of $[FeF_4]^-$, which produces $[FeF_3]^-$ by elimination of a fluorine radical (Figure 2a). $[FeF_3]^-$ is also produced by activating larger cluster ions; for example, CID of $[EMIm]^+[FeF_4]^-_2$ produces a low-abundance ion at *m/z* 113 in addition to the expected $[FeF_4]^-$ formed by elimination of $[EMIm]^+[FeF_4]^-$ (Figure 2b). The $[FeF_3]^-$ measured could also be present in the aqueous phase or could be induced by a reductive process occurring in the electrospray ionization, but subsequent considerations argue against these explanations. Lower abundance ions are seen at *m/z* 103 and 123, which correspond to $[AlF_4]^-$ and $[SiF_5]^-$ [59], an indication of the remarkable ability of the fluorohydrogenate for attacking silicate.

These observations suggest that iron is present in the fluorohydrogenate IL as $[FeF_4]^-$. If the iron existed predominantly as a solvated cation (e.g., as in the case of aqueous solutions) one would expect to see ions containing a statistical distribution of mixed halide ligands formed during evaporation of the electrospray droplets. Since there is little signal from mixed halide complexes, we conclude that the iron exists overwhelming as the $[FeF_4]^-$ fluoroanion in the Fe(III)-ionic liquid system.

Numerous cluster ions are seen in the anion spectrum that consist of one or more $[EMIm^+]$ cations together with combinations of $[Cl^-]$, $[F(HF)^-]$, and/or $[FeF_4^-]$ (Table 1). The most abundant clusters contained $[Cl^-]$ as opposed to $[F(HF)^-]$; the relative intensities of envelope of ions from *m/z* 181 to 189 is illustrative, with $[EMIm^+][Cl^-]_2$ (*m/z* 181)>$[EMIm^+][Cl^-][F(HF)^-]$ (*m/z* 185)>$[EMIm^+][F(HF)^-]_2$ (*m/z* 189). Other cluster ion envelopes display the same trend. This was surprising since the fluorohydrogenate anion forms a more stable complex than the chloride anion in the condensed phase [13]. This experiment was conducted using a 9:1 molar excess of $[EMIm^+][F(HF)_{2.3}^-]$:$FeCl_3$, and a significant fraction of the fluoride may have been consumed in reaction with Fe(III), leaving excess $[Cl^-]$ in solution available for complex formation with $[EMIm^+]$. Cluster ions containing $[FeF_4^-]$ anions are present (Table 1) but in lower abundance than those containing only $[Cl^-]$ anions. This may reflect weaker binding between $[EMIm^+]$ and $[FeF_4^-]$ compared with $[Cl^-]$.

A relatively significant ion was seen at *m/z* 280, which corresponds to $[(CF_3SO_2)_2N]^-$ (triflimide). It is present as a contaminant in the electrospray ionization source as a result of analyses of other ionic liquid systems. Triflimide is remarkably difficult to purge from an electrospray instrument, and so our opinion is that it should be introduced into the mass spectrometer with reticence; on the other hand, it has a large negative mass defect and can serve as an omnipresent mass standard.

With the exception of the cluster anions, the chemical background in the mass spectrum was very low, which suggests that high-accuracy, high-precision isotope ratios might be

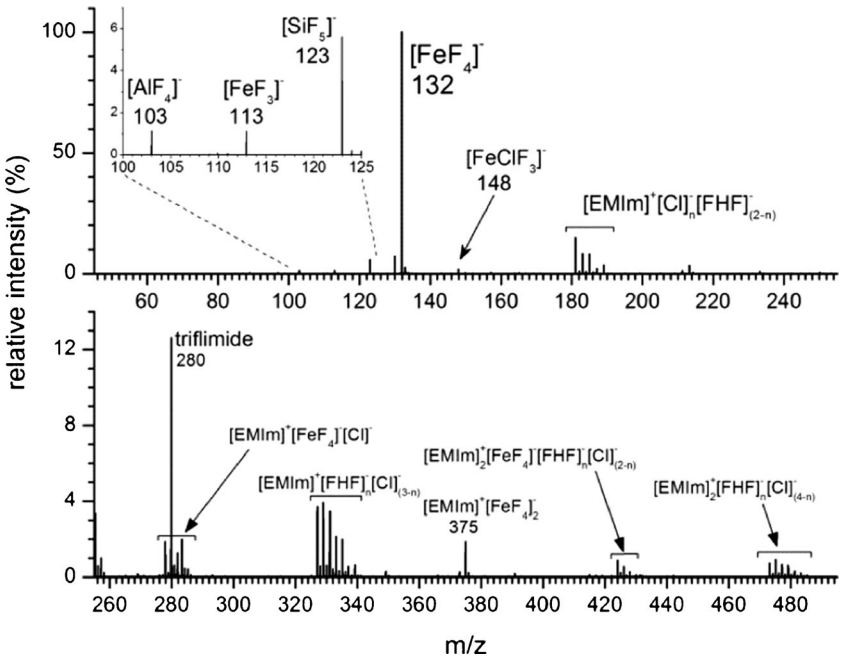

Figure 1. Negative mode electrospray mass spectrum of 10 mM $FeCl_3$ in water diluted 1:9 with 10 mM $[EMIm^+][F(HF)_{2.3}^-]$ in acetonitrile

achievable using this ion formation chemistry. This expectation is supported by isotope ratios measured for both $[FeF_4]^-$ and $[SiF_5]^-$, which showed very good agreement in comparison with theoretical values (Table 2). Better precision and accuracy are no doubt limited by detector response limitations, and mass discrimination in the time-of-flight detector, which are manifest in the baseline around the most intense isotopic ions, viz., $[^{56}FeF_4]^-$ and $[^{28}SiF_5]^-$ (Figure 3). We feel that measurement of the fluoroanion isotopic envelopes using a mass analyzer with dedicated collectors would have the potential for high sensitivity, high accuracy, and high precision.

The positive ion spectrum of $FeCl_3$-$[EMIm]^+[F(HF)_{2.3}]^-$ contained a base peak at *m/z* 111 corresponding to $[EMIm]^+$, and nothing else above 5% relative abundance (Figure 4). The most abundant cluster ion corresponds to $[EMIm]^+_2[F]^-$ at *m/z* 241. In the spectrum of $[EMIm]^+[F(HF)_{2.3}]^-$ by itself, the *m/z*

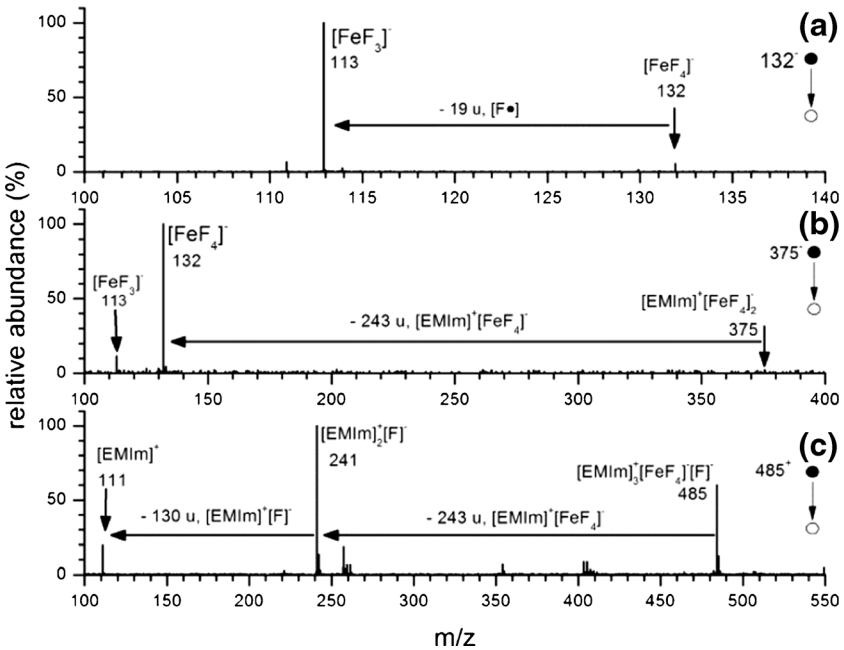

Figure 2. Collision-induced dissociation spectra for the **(a)** negative-ion peak at *m/z* 132 ($[FeF_4]^-$), **(b)** negative-ion peak at *m/z* 375 ($[EMIm]^+[FeF_4]_2^-$), **(c)** positive-ion peak at *m/z* 484 ($[EMIm]^+_3[F]^-[FeF_4]^-$)

Table 1. Ion Compositions for Anions Seen in the Negative Ion Electrospray Spectrum of Acetonitrile Solutions of Iron Chloride Salts Dissolved in $[EMIm]^+[F(HF)_{2.3}]^-$. Monoisotopic *m/z* Values are Listed (i.e., Calculated for ^{35}Cl). Intensity Values are Normalized to 100%

m/z	Composition	% Rel. intensity	*m/z*	Composition	% Rel. intensity
103	$[AlF_4]^-$	2.2	327	$[EMIm]^+_2[Cl]^-_3$	7.2
113	$[FeF_3]^-$	1.0	331	$[EMIm]^+_2[F(HF)]^-[Cl]^-_2$	6.0
123	$[SiF_5]^-$	9.2	335	$[EMIm]^+_2[F(HF)]^-_2[Cl]^-$	3.8
132	$[FeF_4]^-$	100.0	339	$[EMIm]^+_2[F(HF)]^-_3$	1.3
181	$[EMIm]^+[Cl]^-_2$	15.2	375	$[EMIm]^+[FeF_4]^-_2$	3.7
185	$[EMIm]^+[Cl]^-[F(HF)]^-$	8.8	424	$[EMIm]^+_2[FeF_4]^-[Cl]^-_2$	2.2
189	$[EMIm]^+[F(HF)]^-_2$	6.4	428	$[EMIm]^+_2[FeF_4]^-[F(HF)]^-[Cl]^-$	0.8
278	$[EMIm]^+[FeF_4]^-[Cl]^-$	3.1	473	$[EMIm^-]^+_3[Cl]^-_4$	1.7
280	$[(CF_3SO_2)_2N]^-$	25.5	477	$[EMIm]^+_3[F(HF)]^-[Cl]^-_3$	1.5
282	$[EMIm]^+[FeF_4]^-[F(HF)]^-$	2.1			

241 ion is accompanied by $[EMIm]^+_2[F(HF)]^-$ at *m/z* 261 that is nearly as abundant [59]. However, in the $FeCl_3$ experiment the *m/z* 261 ion is very low in abundance, being replaced by $[EMIm]^+_2[Cl]^-$ at *m/z* 257. Other fluorohydrogenate cluster ion congeners are also absent and, instead, higher $[EMIm]^+[Cl]^-$ cluster congeners are seen at *m/z* 403 and 551. As expected, an $[EMIm]^+_2[FeF_4]^-$ cluster is observed at *m/z* 354. The ion at *m/z* 484 nominally corresponds to $[EMIm]^+_3[F]^-[FeF_4]^-$; this composition stands out because in studies of zirconium it was concluded that $[ZrF_6]^{2-}$ was present [60], and by analogy the composition here might be $[EMIm]^+_3[FeF_5]^{2-}$. However, we believe that a better explanation is cluster formation involving the neutral $[EMIm]^+[FeF_4]^-$ clustering with $[EMIm]^+_2[F]^-$ (*m/z* 241), since we do not see other evidence for $[FeF_5]^{2-}$.

While the collision induced dissociation reactions of the positive cluster ions produced $[EMIm]^+$ overwhelmingly (Figure 2b), the CID spectrum of $[EMIm]^+_3[F]^-[FeF_4]^-$ (*m/z* 484, Figure 2c) reveals binding preferences in that at the lowest collision energies $[EMIm]^+[FeF_4]^-$ is eliminated producing $[EMIm]^+_2[F]^-$ at *m/z* 241. This suggests that in this cluster, $[F]^-$ is either very weakly or not at all bound to $[FeF_4]^-$, which, together with the lack of a peak at *m/z* 75.5 (un-clustered $[FeF_5]^{2-}$) in the anion spectrum, argues against the presence of $[FeF_5]^{2-}$. The dissociation process represents the reverse of the clustering reaction proposed for formation of *m/z* 484, and suggests that $[EMIm]^+$ binds more strongly to fluoride compared to $[FeF_4]^-$.

The negative-ion mass spectrum of a solution generated by dissolving the iron(II) salt $FeCl_2$ in water followed by dilution in $[EMIm]^+[F(HF)_{2.3}]^-$/acetonitrile was indistinguishable from the negative-ion mass spectrum generated from an analogous solution containing $FeCl_3$ (Supplementary Figure S1). The base peak was $[FeF_4]^-$, a species in which Fe is in the 3+ oxidation state, and all other cluster ions were identical, with close agreement between the relative abundances seen in the $FeCl_3$ and $FeCl_2$ experiments. Additionally, the positive-ion electrospray of this $FeCl_2/[EMIm]^+[F(HF)_{2.3}]^-$ acetonitrile solution was identical to the positive-ion mass spectrum of the $FeCl_3$/ionic liquid solution, showing no trace of $[EMIm]^+_2[FeF_3]^-$, only $[EMIm]^+_2[FeF_4]^-$ and higher cluster congeners of the same ions. Thus, in marked contrast to the Fe(III) experiment, the oxidation state of the metal is different in the gas phase compared with what is believed to be in solution. Accordingly, it was hypothesized that either the Fe oxidation state in solution was not what was stated, or that Fe(II) is oxidized upon mixture with the $[EMIm]^+[F(HF)_{2.3}]^-$-acetonitrile solution, or by the electrospray process. Benchmark measurements for aqueous Fe(II) and Fe(III) chloride solutions and DFT-calculated energetic difference between $[FeF_3]^-$ and $[FeF_4]^-$ (described below) demonstrated that mixtures of Fe(II) with the fluorohydrogenate solution followed by ESI were in fact oxidizing. The identity of the oxidizing agent is unknown but is hypothesized to be oxygen, likely dissolved in all of the liquids used in these experiments. It is worthwhile noting that the spray chamber is continually flushed with high purity nitrogen, which suggests that atmospheric oxygen cannot be the oxidant; however, it is possible that traces of oxygen are dissolved into the IL. We attempted to remove this by sparging the sample IL with nitrogen, but the results were inconclusive, and the identity of the oxidant remains an open question.

Table 2. Isotope Ratios Measured for $[FeF_4]^-$ and $[SiF_5]^-$, and Compared with Theoretical Values

Composition	*m/z*	% Abundance, relative to ^{56}Fe- or ^{28}Si-containing isotopomers	% Abundance, theoretical
$[^{54}FeF_4]^-$	129.939	6.25±0.58	6.37
$[^{56}FeF_4]^-$	131.934	100	100
$[^{57}FeF_4]^-$	132.935	2.41±0.22	2.31
$[^{58}FeF_4]^-$	133.932	0.39±0.06	0.31
$[^{28}SiF_5]^-$	122.974	100	100
$[^{29}SiF_5]^-$	123.973	5.16±0.57	5.08
$[^{30}SiF_5]^-$	124.970	3.71±0.80	3.35

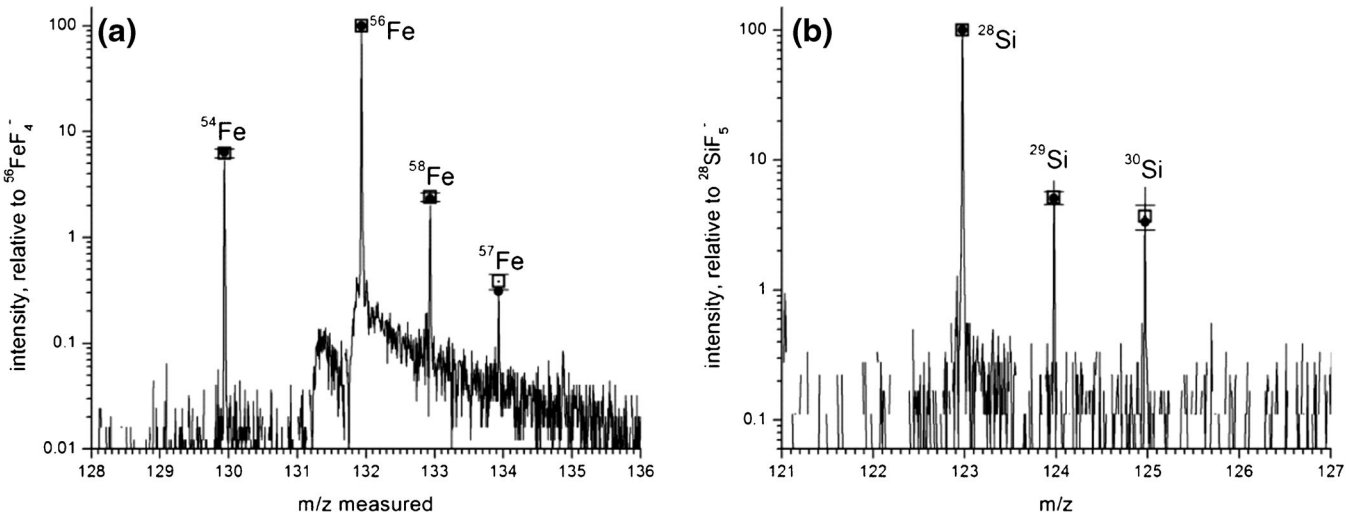

Figure 3. Percent intensity, relative to the most abundant ion in the isotopic envelope. Open squares, with error bars, are measured values. Filled circles are theoretical values. The lines are a representative individual spectrum. **(a)** $[FeF_4]^-$; **(b)** $[SiF_5]^-$

Electrospray Analyses of Iron(III) and Iron(II) Chloride Solutions

Negative electrospray ionization of an aqueous solution of iron(II) chloride dissolved in ACN produced a mass spectrum consisting almost entirely of the $[FeCl_3]^-$ isotopic envelope (Figure 5a); a much lower abundance $[FeCl_4]^-$ envelope was also recorded, but its intensity was <6% of the Fe(II) species. The $[FeCl_4]^-$ is likely derived from Fe(III) in the spray solution, since one would expect reduction, not oxidation reactions to occur at the emitter in negative-ion mode electrospray. Therefore, the overriding conclusion here is that the oxidation state of iron in gas-phase species is the same as that presumed to be in solution.

The spectrum generated by the complementary experiment starting with $FeCl_3$ produced abundant isotopic envelopes corresponding to the expected Fe(III) species $[FeCl_4]^-$ and the Fe(II) species $[FeCl_3]^-$, in a ratio of about 3:1 (Figure 5b). Either the spray solution contains significant Fe(II) or the electrospray process and/or subsequent transfer to vacuum is reducing a significant amount of the Fe(III). A 1000-fold molar excess of hydrogen peroxide relative to Fe(III) was added to the Fe(III) solution (oxidizing any Fe(II) present to the 3+ state), and then electrosprayed; this produced the same spectrum as observed in the analysis of the aqueous $FeCl_3$ solution (Figure 5c), indicating that solution-phase Fe(II) does not make a significant contribution to the appearance of gas-phase Fe(II) species. These experiments suggest that the electrospray signature of Fe(III) chloride consists of $[FeCl_4]^-$ and $[FeCl_3]^-$ in about a 3:1 ratio, and that the $[FeCl_3]^-$ is produced either by a reductive process occurring in the electrospray source or by gas-phase fragmentation of $[FeCl_4]^-$ through the elimination of a chlorine radical (analogous to the fluorine radical elimination seen in CID of $[FeF_4]^-$). In source CID experiments showed that $[FeCl_4]^-$ could be converted to $[FeCl_3]^-$, but this did not begin to occur until an additional 30 eV was applied (Supplementary Figure S2), which suggests that reduction is caused by the electrospray source. The reduction of a fraction of the $[FeCl_4]^-$ contrasts sharply with the oxidative process seen in electrospray ionization of Fe-containing solutions conducted in the presence of $[EMIm]^+[F(HF)_{2.3}]^-$.

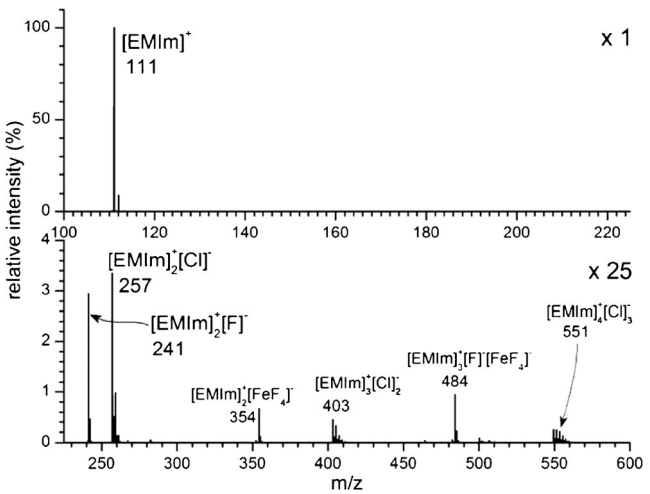

Figure 4. Positive mode electrospray mass spectrum of 10 mM $FeCl_3$ in water diluted 1:9 with 10 mM $[EMIm^+][F(HF)_{2.3}^-]$ in acetonitrile

Computational Studies of the Iron Fluoroanions

Density functional theory calculations were performed in order to understand whether or not there were underlying thermodynamic reasons for the absence of $[FeF_3]^-$-containing complexes, and the nature of the interaction between the iron fluoroanions and the $[EMIm]^+$ cation. The stable structure predicted for $[FeF_3]^-$ was a trigonal pyramid with a quintet electron configuration (a complete list of coordinates calculated for all structures is found in the Supplementary Material). $[FeF_4]^-$ was predicted to be a tetrahedron with a sextet electron

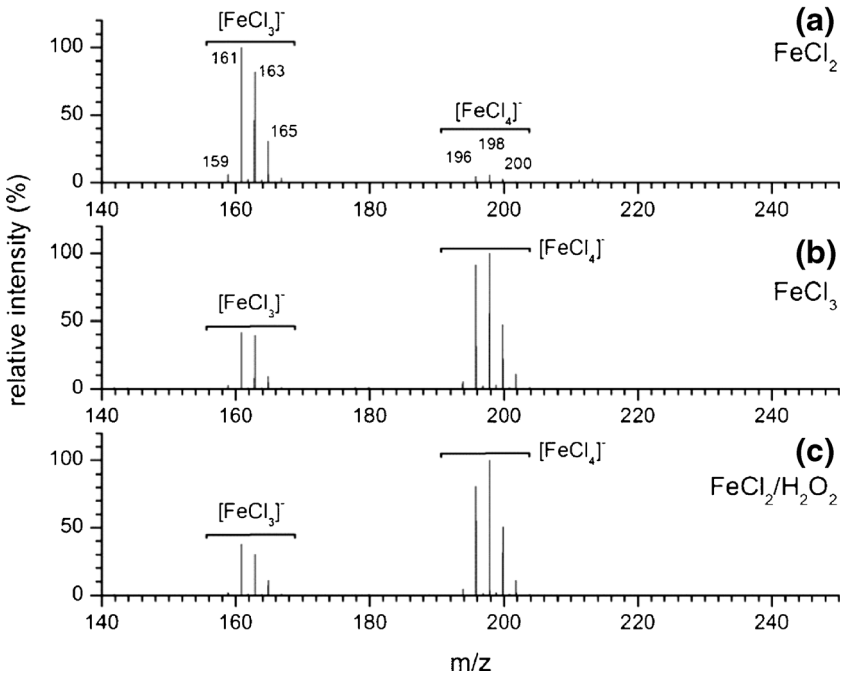

Figure 5. **(a)** Negative mode electrospray mass spectrum of 10 mM $FeCl_2$ in water diluted 1:9 with acetonitrile. **(b)** Negative mode electrospray mass spectrum of 10 mM $FeCl_3$ in water diluted 1:9 with acetonitrile. **(c)** Negative mode electrospray mass spectrum of 10 mM $FeCl_3$ in water mixed with H_2O_2 and diluted 1:9 with acetonitrile

configuration. Energetically, tetrahedral $[FeF_4]^-$ lies 644 kJ/mole below $[FeF_3]^-$+F, although we note that such a reaction is not a reasonable explanation for the high abundance of $[FeF_4]^-$ and the depleted abundance of $[FeF_3]^-$ since fluorine

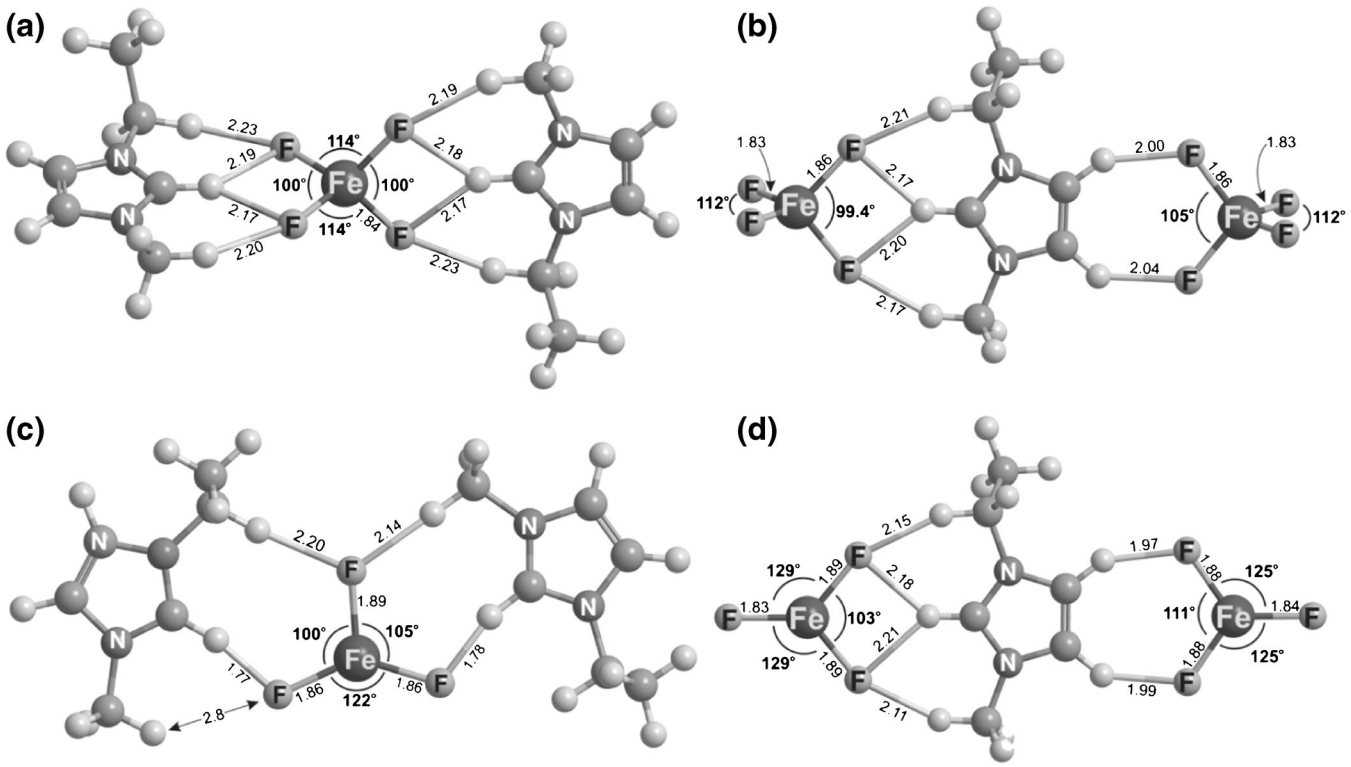

Figure 6. DFT-generated structures for the $[EMIm]^+$ iron fluoride complexes. **(a)** and **(b)** $[FeF_4]^-$ complexes. **(c)** and **(d)** $[FeF_3]^-$ complexes

Table 3. Energetic Values Calculated for the Iron Fluoroanions, Complexes, and Related Species. Values Are in au Unless Stated Otherwise. Density Functional Theory Calculations Were Performed at the B3LYP Level of Theory, with the 6-311++G(d,p) Basis Set for All Atoms

Species (Fe geometry/electronic configuration)	Energy (E+ZPE, hartrees)	Enthalpy (298.15 K, hartrees)	Gibbs free energy (298.15 K, hartrees)	Binding energy (hartrees)	Binding Energy (kJ/mol)
$[F(HF)]^-$ (singlet)	–200.4349	–200.4314	–200.4562		
$[EMIm]^+$ (singlet)	–344.4688	–344.4594	–344.5025		
$[F]^-$ (singlet)	–99.8887				
HF (singlet)	–100.4730	–100.4697	–100.4895		
F (doublet)	–99.7606				
$[FeF_4]^-$ (tetrahedral-sextet)	–1663.4784	–1663.4708	–1663.5089		
$[FeF_3]^-$ (trigonal pyramidal-quintet)	–1563.5492	–1563.5429	–1563.5797		
$[EMIm]^+_2[FeF_4]^-$ (tetrahedral sextet)	–2352.5917	–2352.5637	–2352.6578	0.1757	461
$[EMIm]^+[FeF_4]^-_2$ (tetrahedral sextet)	–3671.5945	–3671.5686	–3671.6568	0.1690	443
$[EMIm]^+_2[FeF_3]^-$ (distorted trigonal planar-quintet)	–2252.6860	–2252.6592	–2252.7526	0.1992	523
$[EMIm]^+[FeF_3]^-_2$ (distorted trigonal planar-quintet)	–3471.7793	–3471.7557	–3471.8395	0.2120	556

atoms are not likely to be present in the electrospray experiments. If neutral FeF_3 were present, complexation with $[F]^-$ might account for formation of the dominant $[FeF_4]^-$ anion, and this is predicted to be exothermic by 432 kJ/mol.

Metal fluoroanions are stable in the fluorohydrogenate ionic liquid, which is consistent with the presence of the anion–cation complexes in the gas phase [19, 21]. We focused DFT modeling on the $[EMIm]^+_2[FeF_4]^-$ and $[EMIm]^+[FeF_4]^-_2$ complexes, comparing these with the analogous $[FeF_3]^-$ species to see whether there were significant differences in interaction energies that might help explain the low abundance of the latter. In the $[EMIm]^+_2[FeF_4]^-$ cationic complex (Figure 6a), the cations are bound to $[FeF_4]^-$ by four F–H bonds involving three H and two F atoms situated in a "W" geometry. The anions preferentially bind with the methyne H atom of the imidazolium ring, which is the most acidic H atom in the cation, and two H atoms on vicinal alkyl groups are also involved.[58] The F–H bond lengths ranged from 2.17 to 2.23 Å for each cation, consistent with hydrogen bonds of intermediate strength. The F–Fe bond lengths are all about 1.83 Å, nearly identical to uncomplexed $[FeF_4]^-$, even though the $[FeF_4]^-$ tetrahedron is slightly distorted in the $[EMIm]^+_2[FeF_4]^-$ cluster, with bond angles of the binding F–Fe–F moieties at 100°, and the non-binding F–Fe–F moieties at about 114°; by way of comparison, the F–Fe–F bond angles in uncomplexed $[FeF_4]^-$ are 109°).

The structure of the anionic complex $[EMIm]^+[FeF_4]^-_2$ displays one of the $[FeF_4]^-$ anions bound to the methyne side of the imidazolium in the same "W" motif, with practically identical F–H and F–Fe bond lengths and F–Fe–F bond angles. The second $[FeF_4]^-$ anion is bound via two F–H bonds involving the acetylenic H atoms; these are significantly shorter at 2.00 and 2.04 Å but there are fewer of them. The geometries of both $[FeF_4]^-$ anions in this complex are very similar to one another.

Calculation of the total cation-anion binding energies produced a value of 461 kJ/mol for $[EMIm]^+_2[FeF_4]^-$ (Table 3, reaction 1), and a very similar value of 443 kJ/mol for $[EMIm]^+[FeF_4]^-_2$ (reaction 2). Based on the structural preference for binding to the methyne H atom displayed by the $[EMIm]^+_2[FeF_4]^-$ cation, modeling of the unsymmetrical $[EMIm]^+[FeF_4]^-_2$ anion was expected to show an energetic preference for elimination of the anion bound to the acetylenic side of the imidazolium ring (Figure 7). DFT modeling suggested that this was energetically favored, by 384 kJ/mol.

$$[EMIm]^+_2[FeF_4]^- \rightarrow 2\,[EMIm]^+ + [FeF_4]^- \quad (1)$$

$$[EMIm]^+[FeF_4]^-_2 \rightarrow [EMIm]^+ + 2[FeF_4]^- \quad (2)$$

Stable complexes were also predicted for $[EMIm]^+_2[FeF_3]^-$ and $[EMIm]^+[FeF_3]^-_2$, with calculated anion–cation complex binding energies of 523 and 556 kJ/mol (reactions 3 and 4, respectively). These values are even higher than those

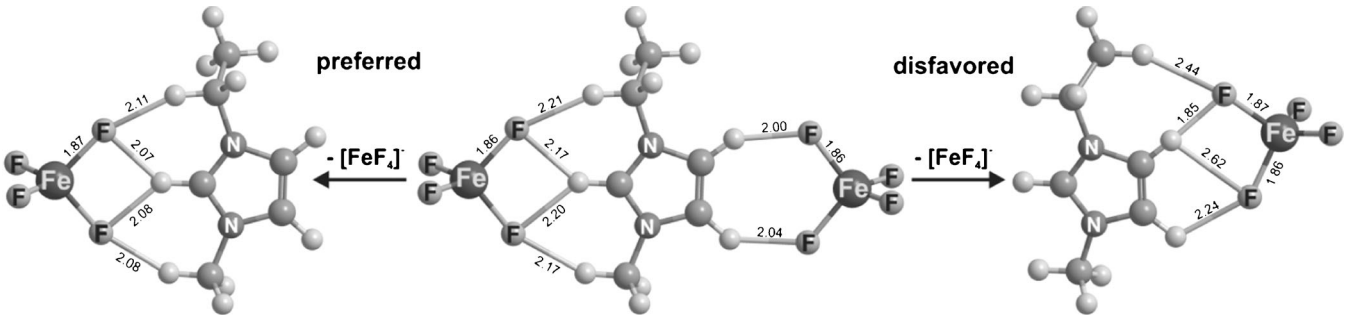

Figure 7. Dissociation pathways for $[EMIm]^+[FeF_4]^-_2$

calculated for the $[FeF_4]^-$-containing complexes, suggesting that if $[FeF_3]^-$ is present, its clusters should form and be observed in the mass spectra. Thus, it is unlikely that Fe(II) is present in the sample solutions generated from the IL and either Fe(II) or Fe(III).

$$[EMIm]^+_2[FeF_3]^- \rightarrow 2[EMIm]^+ + [FeF_3]^- \quad (3)$$

$$[EMIm]^+[FeF_3]^-_2 \rightarrow [EMIm]^+ + 2[FeF_3]^- \quad (4)$$

The structure of $[EMIm]^+_2[FeF_3]^-$ (Figure 6c) contained $[FeF_3]^-$ in a distorted trigonal planar geometry: F–Fe–F angles directed towards the cation are 100° and 105°, significantly smaller than the 120° angle calculated in uncomplexed trigonal planar structure. This geometry is somewhat surprising because the uncomplexed trigonal pyramid with a quintet electronic configuration is 390 kJ/mol lower than the trigonal planar structure as a singlet. Attempts to optimize $[EMIm]^+_2[FeF_3]^-$ (and $[EMIm]^+[FeF_3]^-_2$) with $[FeF_3]^-$ in the trigonal planar geometry with a singlet electronic configuration were not successful, and neither were attempts to calculate a triplet electronic configuration. Although not locating an optimized structure does not rule out the possibility, it likely indicates a preference for the quintet electronic configuration. A true trigonal planar geometry is not allowed for a 3-coordinate d^6 metal as a quintet due to orbital degeneracies. It was surprising that the F–Fe–F moieties having bond angles approaching 100° did not adopt the "W" bonding motif seen in the distorted tetrahedron $[FeF_4]^-$; however, we believe that orienting the methyne H atom into the center of the F–Fe–F cleft would result in cation-cation repulsion. The bidentate interaction results in a complex that that is actually more stable than those formed from via the "W" bonding motif.

Comparing the $[EMIm]^+_2[FeF_3]^-$ structure with that of the analogous $[FeF_4]^-$-containing complex, the weaker F–H bonds in the $[FeF_3]^-$-containing molecule have approximately the same bond lengths as do all of the F–H bonds in the $[FeF_4]^-$-containing complex. However, there in nothing in the latter comparable to the short 1.77–1.78 Å bonds seen in the $[FeF_3]^-$ complexes and, hence, it is probable that these are primarily responsible for the higher anion–cation binding energy of the $[FeF_3]^-$ complex (523 compared with 461 kJ/mol for the $[FeF_4]^-$ complex].

In case of the $[EMIm]^+[FeF_3]^-_2$ complex, cation repulsion is not an issue, and one $[FeF_3]^-$ moiety does adopt "W" bonding via four F–H bonds ranging from 2.11 to 2.21 Å involving the methyne H atom and H atoms from the pendant alkyl groups (Figure 6d). In this environment, the bonding F–Fe–F moiety has a bond angle of 103°, just slightly greater than the values calculated for the complexes $[FeF_4]^-$ anions. However, the calculations suggest that "W"-bonding would likely not be possible with an F–Fe–F angle greater than about 103°. The second $[FeF_3]^-$ anion binds with the acetylenic H atoms via two F–H bonds (1.97 and 1.99 Å), just like it does in the $[EMIm]^+[FeF_4]^-_2$ complex. This interaction also causes some distortion of the trigonal planar geometry, but the bond angle of the binding F–Fe–F moiety is only reduced to 111°. The atoms comprising the imidazolium ring and the atoms of both $[FeF_3]^-$ anions are practically co-planar, and this was the case for the $[EMIm]^+_2[FeF_3]^-$ complex as well. The anion–cation binding energy in $[EMIm]^+[FeF_3]^-_2$ is significantly greater compared with the analogous $[EMIm]^+[FeF_4]^-_2$ complex (556 versus 443 kJ/mol), which is surprising given that both complexes have similar bonding.

Conclusions

The $[FeF_4]^-$ fluoroanion can be formed in abundance by ESI of a dilute solution of the fluorohydrogenate IL $[EMIm]^+[(HF)_{2.3}F]^-$ containing either Fe(II) or Fe(III). In the Fe(II)-IL experiment, iron is oxidized, a result that contrasts with ESI of aqueous Fe(II) or Fe(III) (with no IL present) in which the oxidation state of iron is preserved or partially reduced as the complexes are transferred into the gas phase. The result is consistent with the thermodynamic advantage gained in forming $[FeF_4]^-$, even though an oxidizing agent has not yet been identified. Interaction with the imidazolium cation increases the stability of the $[FeF_4]^-$ anion in the condensed phase ionic liquid, which in turn leads to enhanced formation of gas-phase $[FeF_4]^-$. The mass spectra generated by these experiments have low background and no isobaric interferences, characteristics that are favorable for accurate measurements of isotope ratios of iron samples. This result,

together with prior demonstrations of the formation of EMIm-fluorohydrogenate ionic liquids containing B, P, As, Nb, Ta, W, and U, and the recent observation of Zr and Si fluoroanions by electrospray, suggests that this approach will have wide applicability for forming metal fluoroanions, not only for isotope ratio measurements but also for gas-phase ion chemistry studies.

References

1. Peryshkov, D.V., Goreshnik, E., Mazej, Z., Strauss, S.H.: Co-crystallization of octahedral and icosahedral fluoroanions in $K_3(AsF_6)(B_{12}F_{12})$ and $Cs_3(AsF_6)(B_{12}F_{12})$. Rare examples of salts containing fluoroanions with different shapes and charges. J. Fluor. Chem. **131**, 1225–1228 (2010)
2. Sharma, R.P., Singh, A., Venugopalan, P., Harrison, W.T.A.: Binding of fluoroanions by a cationic cobalt(III) complex: syntheses, characterization and single crystal X-ray structure determination of $Co(phen)_2CO_3$ BF_4 and $Co(phen)_2CO_3$ $PF_6.3H_2O$. J. Mol. Struct. **994**, 6–12 (2011)
3. Sharma, R., Sharma, R.P., Kariuki, B.M.: Second sphere interaction in fluoroanion binding: Synthesis, spectroscopic and X-ray structural study of trans-dichlorobis (ethylenediamine) cobalt(III) terafluoroborate. J. Fluor. Chem. **129**, 325–331 (2008)
4. Sharma, R.P., Singh, A., Brandao, P., Felix, V., Venugopalan, P.: Second sphere coordination in binding of fluoroanions: synthesis, spectroscopic characterization, and single crystal X-ray structure determination of $Co(phen)_3(BF4)_3$-H_2O and $Co(phen)_3(PF6)_3$-CH_3COCH_3. J. Mol. Struct. **920**, 119–127 (2009)
5. Sharma, R.P., Sharma, R., Bala, R., Rychlewska, U., Warzajtis, B., Ferretti, V.: Second-sphere coordination complexes via hydrogen bonding: Synthesis, spectroscopic characterization, crystal structures and packing of cis-diazidobis(ethylenediamine)cobalt(III) cations with complex fluoroanions. J. Mol. Struct. **753**, 182–189 (2005)
6. Sharma, R.P., Singh, A., Venugopalan, P., Ferretti, V.: Binding of fluorine containing anions by new cationic Co(III) complex: competitive interaction of chloride and hexafluorophosphate with $Co(phen)(H_2biim)_2^{3+}$. J. Fluor. Chem. **132**, 453–458 (2011)
7. Petrosyants, S.P., Ilyukhin, A.B...: Ensembles of indium and gallium fluoroanions with HF molecules and bipyridine cations. Rus. J. Inorg. Chem. **56**, 1250–1257 (2011)
8. Radan, K., Lozinsek, M., Goreshnik, E., Zemva, B.: Syntheses, structures, and Raman spectra of $Cd(BF_4)(AF_6)$ (A = Ta, Bi) compounds. J. Fluor. Chem. **132**, 767–771 (2011)
9. Semeril, D., Matt, D., Harrowfield, J., Schultheiss, N., Toupet, L. Supramolecular chemistry of fluoroanions: selectivity in weak interactions. Dalton Trans. 6296–6298 (2009)
10. Beattie, C., Farina, P., Levason, W., Reid, G.: Oxa-thia-, oxa-selena, and crown ether macrocyclic complexes of tin(II) tetrafluoroborate and hexafluorophosphate - synthesis, properties and structures. Dalton Trans. **42**, 15183–15190 (2013)
11. Kanatani, T., Matsumoto, K., Hagiwara, R.: Syntheses and physicochemical properties of new ionic liquids based on the hexafluorouranate anion. Chem. Lett. **38**, 714–715 (2009)
12. Peryshkov, D.V., Friedemann, R., Goreshnik, E., Mazej, Z., Seppelt, K., Strauss, S.H.: Anion packing, hole filling, and HF solvation in $A_2(HF)_nB_{12}F_{12}$ and $K_2(HF)TiF_6$ (A = K, Cs). J. Fluor. Chem. **145**, 118–127 (2013)
13. Hagiwara, R., Hirashige, T., Tsuda, T., Ito, Y.: Acidic 1-ethyl-3-methylimidazolium fluoride: a new room temperature ionic liquid. J. Fluor. Chem. **99**, 1–3 (1999)
14. Hagiwara, R., Hirashige, T., Tsuda, T., Ito, Y.: A highly conductive room temperature molten fluoride: EMIF-2.3HF. J. Electrochem. Soc. **149**, D1–D6 (2002)
15. Hagiwara, R., Ito, Y.: Room temperature ionic liquids of alkylimidazolium cations and fluoroanions. J. Fluor. Chem. **105**, 221–227 (2000)
16. Hagiwara, R., Matsumoto, K., Nakamori, Y., Tsuda, T., Ito, Y., Matsumoto, H., Momota, K.: Physicochemical properties of 1,3-dialkylimidazolium fluorohydrogenate room-temperature molten salts. J. Electrochem. Soc. **150**, D195–D199 (2003)
17. Hagiwara, R., Matsumoto, K., Tsuda, T., Ito, Y., Kohara, S., Suzuya, K., Matsumoto, H., Miyazaki, Y.: The structures of alkylimidazolium fluorohydrogenate molten salts studied by high-energy X-ray diffraction. J. Non-Crystal. Solids **312/14**, 414–418 (2002)
18. Hagiwara, R., Nakamori, Y., Matsumoto, K., Ito, Y.: The effect of the anion fraction on the physicochemical properties of $EMIm(HF)_nF$ (n = 1.0–2.6). J. Phys. Chem. B **109**, 5445–5449 (2005)
19. Matsumoto, K., Hagiwara, R.: A new room temperature ionic liquid of oxyfluorometallate anion: 1-ethyl-3-methylimidazolium oxypentafluorotungstate ($EMImWOF_5$). J. Fluor. Chem. **126**, 1095–1100 (2005)
20. Matsumoto, K., Hagiwara, R.: Structural characteristics of alkylimidazolium-based salts containing fluoroanions. J. Fluor. Chem. **128**, 317–331 (2007)
21. Matsumoto, K., Hagiwara, R., Ito, Y.: Room temperature molten fluorometallates: 1-ethyl-3-methylimidazolium hexafluoroniobate(V) and hexafluorotantalate(V). J. Fluor. Chem. **115**, 133–135 (2002)
22. Matsumoto, K., Hagiwara, R., Ito, Y., Kohara, S., Suzuya, K.: Structural analysis of 1-ethyl-3-methylimidazolium bifluoride melt. Nucl. Inst. Methods Phys. Res. B **199**, 29–33 (2003)
23. Matsumoto, K., Hagiwara, R., Yoshida, R., et al.: Syntheses, structures and properties of 1-ethyl-3-methylimidazolium salts of fluorocomplex anions. Dalton Trans. 144–149 (2004)
24. Matsumoto, K., Tsuda, T., Hagiwara, R., Ito, Y., Tamada, O.: Structural characteristics of 1-ethyl-3-methylimidazolium bifluoride: HF-deficient form of a highly conductive room temperature molten salt. Solid State Sci. **4**, 23–26 (2002)
25. Saito, Y., Hirai, K., Matsumoto, K., Hagiwara, R., Minamizaki, Y.: Ionization state and ion migration mechanism of room temperature molten dialkylimidazolium fluorohydrogenates. J. Phys. Chem. B **109**, 2942–2948 (2005)
26. Tsuda, T., Hagiwara, R.: Chemistry in heterocyclic ammonium fluorohydrogenate room-temperature ionic liquid. J. Fluor. Chem. **129**, 4–13 (2008)
27. Yoshino, H., Matsubara, S., Oshima, K., Matsumoto, K., Hagiwara, R., Ito, Y.: Halofluorination of alkenes with ionic liquid $EMIMF(HF)_{2.3}$. J. Fluor. Chem. **125**, 455–458 (2004)
28. Yoshino, H., Nomura, K., Matsubara, S., Oshima, K., Matsumoto, K., Hagiwara, R., Ito, Y.: A mild ring opening fluorination of epoxide with ionic liquid 1-ethyl-3-methylimidazorium oligo hydrogenfluoride ($EMIMF(HF)_{2.3}$). J. Fluor. Chem. **125**, 1127–1129 (2004)
29. Zemva, B.: Protonic superacid anhydrous hydrogen fluoride as a solvent in the chemistry of high oxidation states. [Comptes Rendus De L Academie Des Sciences Serie Ii Fascicule C-Chimie] **1**, 151–156 (1998)
30. Gnann, R.Z., Wagner, R.I., Christe, K.O.: Direct syntheses of tetramethylammonium salts of complex fluoroanions. J. Fluor. Chem. **83**, 191–194 (1997)
31. Dukat, W.W., Holloway, J.H., Hope, E.G., Rieland, M.R., Townson, P.J., Powell, R.L.: High oxidation-state binary transition-metal fluorides as selective fluorinating agents. J. Chem. Soc. Chem. Commun. 1429–1430 (1993)
32. Kuhn-Velten, J., Bodenbinder, M., Brochler, R., Hagele, G., Aubke, F.: A F-19 nuclear magnetic resonance study of the conjugate Bronsted-Lewis superacid HSO_3F-SbF_5. Part II. Can. J. Chem. **80**, 1265–1277 (2002)
33. Culmann, J.C., Fauconet, M., Jost, R., Sommer, J.: Fluoroanions and cations in the HF-SbF_5 superacid system. A F-19 and H-1 NMR study. New J. Chem. **23**, 863–867 (1999)
34. Zhang, X.Z., Seppelt, K.: Preparation and structures of salts with the anions of IF_2^-, ClF_4^-, IF_4^-, TeF_7^-, and AsF_4^-. Z Anorg Allg Chem **623**, 491–500 (1997)
35. Brisdon, A.K., Holloway, J.H., Hope, E.G., Levason, W., Ogden, J.S., Saad, A.K.: Metal K-edge extended X-ray absorption fine-structure studies of MOF_6, RuF_6, RhF_6, and related fluoroanions. J. Chem. Soc. Dalton Trans. 447–449 (1992)
36. Brisdon, A.K., Holloway, J.H., Hope, E.G., Levason, W., Ogden, J.S., Saad, A.K.: Metal LIII-edge extended X-ray absorption fine-structure of 5d transition-metal hexafluorides and related fluoroanions. J. Chem. Soc. Dalton Trans. 139–143 (1992)
37. Graudejus, O., Wilkinson, A.P., Chacon, L.C., Bartlett, N.: M-F interatomic distances and effective volumes of second and third transition series MF_6^- and MF_6^{2-} anions. Inorg. Chem. **39**, 2794–2800 (2000)

38. Zhao, X.L., Kieser, W.E., Dai, X., Priest, N.D., Kramer-Tremblay, S., Eliades, J., Litherland, A.E.: Preliminary studies of Pu measurement by AMS using PuF_4. Nucl. Inst. Methods Res B **294**, 356–360 (2013)
39. Zhao, X.-L., Litherland, A.E.: Studies of anions from sputtering II: ^{99}Tc and ^{99}Ru. Nucl. Inst. Methods Res. B **268**, 812–815 (2010)
40. Zhao, X.-L., Litherland, A.E., Eliades, J., Kieser, W.E.: Studies of anions from sputtering I: survey of MF_n^-. Nucl. Instr. Methods Phys. Res. B **268**, 807–811 (2010)
41. Hogan Jr., C.J., Fernandez de la Mora, J.: Ion-pair evaporation from ionic liquid clusters. J. Am. Soc. Mass Spectrom. **21**, 1382–1386 (2010)
42. Jackson, G.P., Duckworth, D.C.: Electrospray mass spectrometry of undiluted ionic liquids Chem. Commun. 522–523 (2004)
43. Dyson, P.J., Khalaila, I., Luettgen, S., McIndoe, J.S., Zhao, D.B.: Direct probe electrospray (and nanospray) ionization mass spectrometry of neat ionic liquids. Chem. Commun. 2204–2205 (2004)
44. Chiu, Y.H., Gaeta, G., Levandier, D.J., Dressler, R.A., Boatz, J.A.: Vacuum electrospray ionization study of the ionic liquid. Int. J. Mass Spectrom. **265**, 146–158 (2007)
45. Lozano, P., Martinez-Sanchez, M.: Ionic liquid ion sources: suppression of electrochemical reactions using voltage alternation. J. Colloid Interface Sci. **280**, 149–154 (2004)
46. Fujiwara, Y., Saito, N., Nonaka, H., Nakanaga, T., Ichimura, S.: A new cluster-ion-beam source for secondary ion mass spectrometry (SIMS) using the electrospray of a pure ionic liquid under high vacuum. Nucl. Inst. Methods Phys. Res. B **268**, 1938–1941 (2010)
47. Fujiwara, Y., Saito, N., Nonaka, H., Nakanaga, T., Ichimura, S.: Characteristics of a charged-droplet beam generated by vacuum electrospray of an ionic liquid Chem. Phys. Lett. **501**, 335–339 (2011)
48. Fujiwara, Y., Watanabe, K., Nonaka, H., Saito, N., Suzuki, A., Fujimoto, T., Kurokawa, A., Ichimura, S.: Metal cluster complex primary ion beam source for secondary ion mass spectrometry (SIMS). Vacuum **84**, 544–549 (2009)
49. Fujiwara, Y., Watanabe, K., Saito, N., et al.: Ion beam generation from an electrolyte solution containing polyatomic cations and anions for secondary ion mass spectrometry. Jpn. J. Appl. Phys. **48**, 126005–10 (2009)
50. Lu, Y.C., King, F.L., Duckworth, D.C.: Electrochemically-induced reactions of hexafluorophosphate anions with water in negative ion electrospray mass spectrometry of undiluted ionic liquids. J. Am. Soc. Mass Spectrom. **17**, 939–944 (2006)
51. Shkrob, I.A., Marin, T.W., Chemerisov, S.D., Hatcher, J.L., Wishart, J.F.: Radiation induced redox reactions and fragmentation of constituent ions in ionic liquids. 2. Imidazolium cations. J. Phys. Chem. B **115**, 3889–3902 (2011)
52. Henderson, M.A., McIndoe, J.S.: Ionic liquids enable electrospray ionisation mass spectrometry in hexane. Chem. Commun. 2872–2874 (2006)
53. Alfassi, Z.R., Huie, R.E., Milman, B.L., Neta, P.: Electrospray ionization mass spectrometry of ionic liquids and determination of their solubility in water. Anal. Bioanal. Chem. **377**, 159 (2003)
54. Stockmann, T.J., Lu, Y., Zhang, J., Girault, H.H., Ding, Z.F.: Interfacial complexation reactions of Sr2+ with octyl(phenyl)-N, N-diisobutylcarbamoylmethylphosphine oxide for understanding its extraction in reprocessing spent nuclear fuels. Chem. Eur. J. **17**, 13206–13216 (2011)
55. Murali, M.S., Bonville, N., Choppin, G.R.: Uranyl ion extraction into room temperature ionic liquids: species determination by ESI and MALDI-MS. Solvent Extr. Ion Exch. **28**, 495–509 (2010)
56. Dyson, P.J., McIndoe, J.S., Zhao, D.B.: Direct analysis of catalysts immobilised in ionic liquids using electrospray ionisation ion trap mass spectrometry Chem. Commun. 508–509 (2003)
57. Zhao, D.B.: Analysis of ionic liquids and dissolved species by electrospray ionization MS. Aust. J. Chem. **57**, 509–509 (2004)
58. Fernandes, A.M., Rocha, M.A.A., Freire, M.G., Marrucho, I.M., Coutinho, J.A.P., Santos, L.: Evaluation of Cation–anion interaction strength in ionic liquids. J. Phys. Chem. B **115**, 4033–4041 (2011)
59. Groenewold, G.S., Delmore, J.E., Benson, M.T., Tsuda, T., Hagiwara, R.: Fluorohydrogenate cluster ions in the gas phase: electrospray ionization mass spectrometry of the [1-ethyl-3-methylimidazolium$^+$][$F(HF)_{2.3}^-$] ionic liquid. J. Phys. Chem. A **117**, 14191–14199 (2013)
60. Groenewold, G.S., Delmore, J.E., Benson, M.T., Tsuda, T., Hagiwara, R.: Generation of gas-phase zirconium fluoroanions by electrospray of an ionic liquid. Rapid Commun. Mass Spectrom. **28**, 1233–1242 (2014)
61. Frisch, M.J., Trucks, G.W., Schlegel, H.B., et al.: Gaussion 03, Rev. C.02. Gaussian, Inc., Wallingford (2004)
62. Parr, R.G., Yang, W.: Density Functional Theory of Atoms and Molecules. Oxford University Press, New York (1989)
63. Becke, A.D.: Density-functional exchange-energy approximation with correct asymptotic-behavior. Phys. Rev. A **38**, 3098–3100 (1988)
64. Lee, C.T., Yang, W.T., Parr, R.G.: Development of the Colle-Salvetti correlation-energy formula into a functional of the electron-density. Phys. Rev. B **37**, 785–789 (1988)